A highly miniturized single-chip MOEMS scanner for all-in-one imaging solution

Jovic, Aleksandar; Uto, Toshihiko; Hei, Kefei; Sancho, Juan; Sanchez, Nuria; Zinoviev, Kirill; Rubio, Jose L.; Margallo, Eduardo; Pandraud, Gregory; Sarro, Pasqualina M.

DOI
10.1109/MEMSYS.2018.8346472

Publication date
2018

Document Version
Final published version

Published in
2018 IEEE Micro Electro Mechanical Systems, MEMS 2018

A HIGHLY MINITURIZED SINGLE-CHIP MOEMS SCANNER FOR ALL-IN-ONE IMAGING SOLUTION

Aleksandar Jovic[1], Toshihiko Uto[2], Kefei Hei[1], Juan Sancho[3], Nuria Sanchez[3], Kirill Zinoviev[4], Jose L. Rubio[3], Eduardo Margallo[3], Gregory Pandraud[1] and Pasqualina M. Sarro[1]

[1]Delft University of Technology, Delft, THE NETHERLANDS

[2]Kaneka, JAPAN, [3]MedLumics, SL., Madrid, SPAIN, [4]IMEC, Heverlee, BELGIUM

ABSTRACT

A highly miniaturized, single-chip, large scanning range MOEMS scanner is demonstrated. This intrinsically-aligned, monolithically integrated device uses small angular displacement to provide a linear scanning range of 2000 µm in the lateral and 1000 µm in the vertical direction, at a working distance of 2 cm, with an average operating power lower than 170 mW. Within a footprint of only 7×10 mm^2, the presented system fully integrates a photonic interferometer comprising a mirror, a silicon microlens and the MEMS actuator into a single chip, thus offering an unprecedentedly miniaturized scanning solution. The monolithic integration of all photonic components provides intrinsic alignment and excludes coupling losses often encountered in systems composed of discrete parts. No additional attenuation of the optical signal is observed during device operation. This small and high-performance device is suitable as complete system-on-chip for commercial, portable imaging applications.

INTRODUCTION

Optical scanners are extensively used devices in metrology and biomedical imaging. Particularly for their use in the medical field, it is highly desirable to make these instruments portable. Therefore, it is relevant to further miniaturize them, so to reduce size, weight, power consumption, without compromising performance. Furthermore, manufacturing techniques suitable for large scale production are preferred to make them affordable.

The need for miniaturization and compactness of optical devices has brought MEMS technology to photonic components like tunable optical filters, lenses and movable mirrors [1]. In particular, MEMS micromirrors are almost irreplaceable components in optical scanners nowadays, especially for interferometric techniques such as optical coherence tomography.

In general, optical imaging and metrology techniques use an interferometer setup as the one schematically depicted in Fig. 1a. The setup consists of several discrete components—such as a light source, a detector, a beam splitter, a reference mirror and an optical scanner—all connected with optical fibers. To achieve the required high performance, complicated and time-consuming assembly procedures are needed, which are largely responsible for the high cost of these systems [2].

Silicon based microtechnology allows wafer scale fabrication of integrated components on a single chip. Each discrete component from Fig. 1a can be implemented in a Si-based photonic integrated circuit (PIC). Optical fibers and beam splitters are replaced by waveguides and multi-modal interferometers [3], and reference mirrors by time delay lines [4]. The light detector can be replaced by integrated photodiodes [5]; and if a spectral analysis is required, photodiodes can be used with an integrated array waveguide grating [6]. Furthermore, with the hybrid integration of a III-V light source [7] on Si, it is possible to fabricate a fully functional interferometric chip, though without scanning functionality.

Scanning can be achieved by moving the light beam with a mirror (Fig. 1b) or by moving the lens (Fig. 1c). Both configurations are enabled by discrete components, but the complexity of the scanner with movable lens is lower [8]. Even an elegant MEMS fiber scanning solution [9] does not exclude the need for complex micro-assembly procedures.

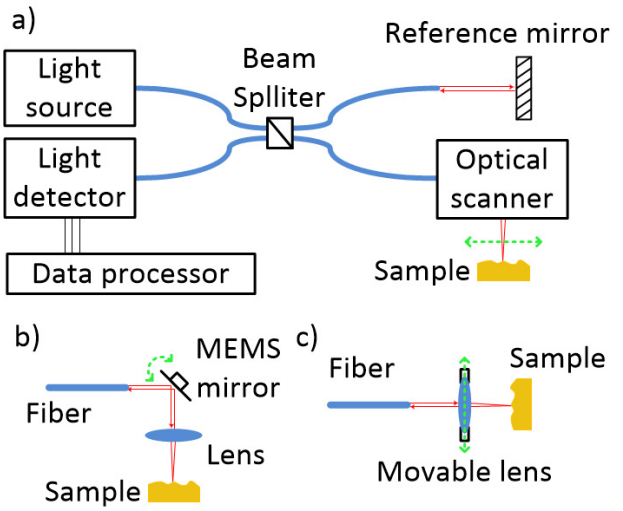

Figure 1: (a) Interferometer configuration for metrology and imaging application. Optical scanner configuration with (b) movable MEMS mirror or (c) movable lens (c).

Although, most of the components from Fig. 1a have already been demonstrated in Si-based integrated technology, no integrated scanner has been reported yet. In this paper we present a highly miniaturized, single-chip MOEMS scanner for OCT which integrates a Si-based passive photonic circuit for the Michelson interferometer, a mirror, a Si microlens [10] and a MEMS actuators system [11] into a standalone device. First, the concept and the system design are introduced. Next, the integration of different submodules is briefly explained, and finally the MOEMS device performance is presented and discussed.

THE SINGLE-CHIP MOEMS SCANNER CONCEPT AND WORKING PRINICPLE

The presented single-chip MOEMS scanner is based on the original concept given in [12]. A waveguide ending with a 45° facet scatters the light towards a microlens at the backside of the wafer. All three components are integrated together into a single Si block, thus ensuring their

intrinsic alignment (Fig. 2a). The rotation of the Si block directly causes the light beam passing through it to scan the incident surface. Hence optical scanning is provided by the angular motion of the Si block, where Δ on the scanned surface is defined by the angular displacement α of the Si block and the working distance of the system w_d according to $\Delta = w_d \times \tan(\alpha)$ (Fig. 2b and Fig. 2c). The conceived design makes it thus possible to achieve large surface scanning with a small α and long w_d (Fig. 4c).

In addition, depending on the application the microlens can be fabricated to be a collimating or a focusing lens. The advantage of the focusing lens is that all optical power is concentrated in a single point, but w_d is predefined by the lens characteristics. On the other hand, with a collimated beam w_d can be easily varied to achieve the desired scanning range.

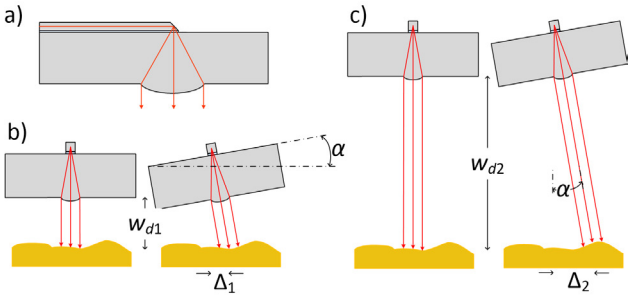

Figure 2: (a) Intrinsically aligned waveguide, mirror and lens integrated in one Si block. (b) Short working distance scanning resulting in a corresponding scanning distance Δ_1 (c) Long working distance scanning, resulting in a larger scanning distance Δ_2.

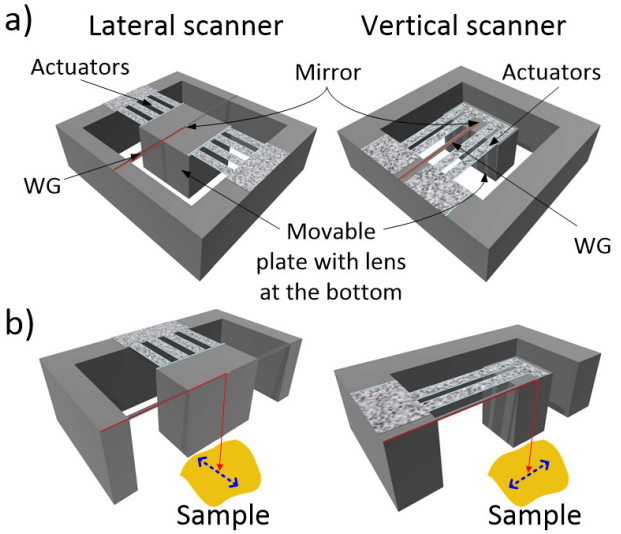

Figure 3: (a) Integrated MOEMS scanners design. (b) Light propagation through the scanners.

Figure 3 depicts the two integrated MOEMS scanners (one for lateral and one for vertical scanning direction) which integrate a waveguide, a 45° mirror facet and a Si microlens into one Si block, which is actuated by electrothermal Al-SiO_2 bimorph beams. The MEMS actuator systems and the working principle are presented in [11]. The light propagation through the scanners is illustrated in Fig. 3b.

SUBMODULES INTEGRATION

The single-chip MOEMS scanner consists of three main submodules: lens, waveguide with mirror facet and MEMS actuator system. The co-fabrication of the submodules is based on the merging of their respective, previously reported process flows [11, 12], further optimized to be mutually compatible.

The process starts with double side-polished silicon on insulator (DP SOI) wafers. First, the front side is protected from mechanical scratches during backside processing with a 1 µm-thick plasma enhanced chemical vapor deposited (PECVD) SiO_2 layer. The Si microlens is fabricated on the wafer backside by transferring an 18 µm high ball cap of reflowed photoresist into Si using a dry etching process (Fig. 4a). The lens surface is smoothened by wet thermal growth of 2.5 µm-thick SiO_2 which is then removed in a buffered 1:7 HF etch solution. A 1 µm thick PECVD SiN layer is then added as a scratch protection of the lens during the following steps (Fig. 4b).

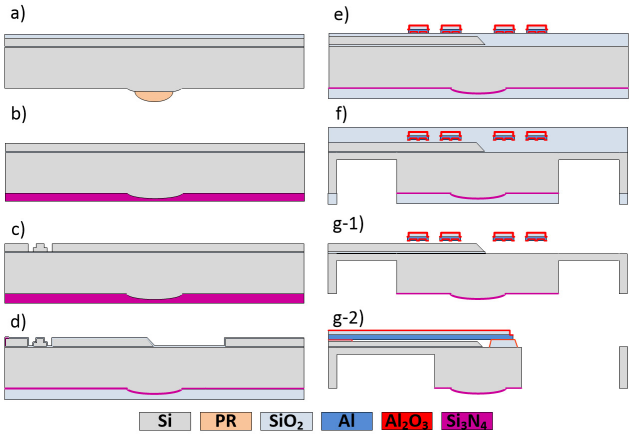

Figure 4: Fabrication process. (a) Shape transfer of reflowed photoresist ball cap to Si using a Si dry etch process. (b) Smoothened microlens with PECVD SiN scratch protection. (c) Two-step waveguide etching process. (d) Mirror etching, sidewall surface roughness reduction, LPCVD SiO_2 cladding, LPCVD SiN antireflecting coating and ALD Al_2O_3 protective layer. (e) Al-SiO_2 bimorph formation using sputtered Al and PECVD SiO_2, protected by ALD Al_2O_3; (f) Backside DRIE etching and hinge formation; (g-1): Vertical scanner (g-2): Lateral scanner device release using vapor HF.

The waveguide circuitry with the mirror is fabricated in the device layer of the DP SOI wafer. The waveguide is fabricated using a 1.8 µm and 1.2 µm deep two-step etching process (Fig. 4c). A 300 nm-thick low pressure chemical vapor deposited LPCVD SiO_2 is deposited as a hard mask for mirror facet formation at the end of the waveguide fabrication process. For this a 25% TMAH and Triton-X-100 mixture is employed. Next, the backside SiN layer is removed in a H_3PO_4 solution at 157 °C, and an additional 500 nm-thick thermal oxide is grown and subsequently removed by wet etching to reduce mirror and waveguide surface roughness at once. A 165 nm-thick LPCVD SiN antireflective coating, a 220 nm-thick LPCVD SiO_2 waveguide cladding layer deposition, and a 20 nm of atomic layer deposited Al_2O_3 (for SiO_2 protec-

tion in the final vapor HF release step) are then added on both wafer sides. Subsequently, the lens is protected by a 5 µm-thick PECVD SiO_2 layer which also serves as a hard mask for the backside deep reactive ion etching (DRIE) of silicon (Fig. 4d).

The final part of the single-chip MOEMS scanner is the fabrication of the MEMS actuators. Both Si device and buried SiO_2 layers are previously removed from the area where the MEMS actuators are built. First, Al-SiO_2 bimorph cantilevers are formed using 2 µm-thick sputtered Al and 2 µm-thick PECVD SiO_2 protected by 200 nm-thick atomic layer deposited Al_2O_3 (Fig. 4e). The devices are then defined by a front side (100 µm) and a two-step backside DRIE (50 µm and 640 µm deep, respectively) for hinge formation (Fig. 4f). The devices are finally released in HF vapor (Fig. 4g). More details on the actuator system fabrication can be found in [16].

An optical image of a fabricated chip with the integrated MOEMS scanner and the interferometer is presented in Fig. 5a. The total footprint of both lateral and vertical MOEMS scanners with interferometer included is 7×10 mm^2. The Si microlens cannot be seen since it is on the backside of the chip. An optical image of the lens with antireflecting coating is shown in Fig. 5b, while a SEM image of the mirror facet at the end of the waveguide is reported in Fig. 5c. Fig. 5d and 5e show SEM images of the interferometer waveguide entry facet and of a S-bend waveguide of the interferometer, respectively.

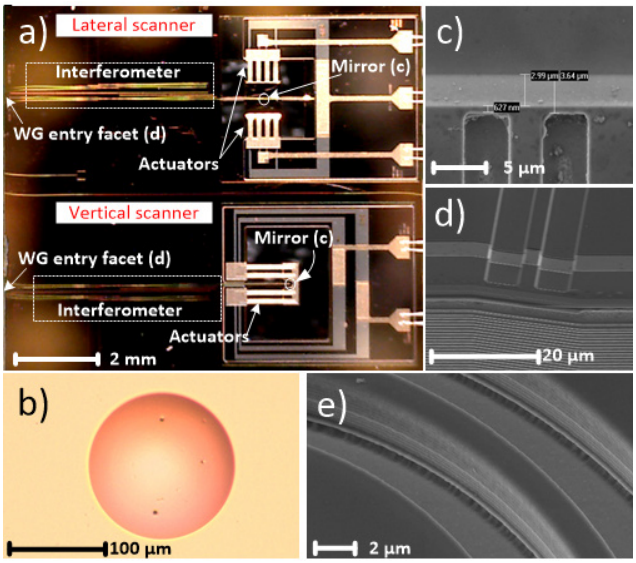

Figure 5: (a) An optical image of the integrated MOEMS scanner and the interferometer on a single chip. (b) The Si microlens with SiN antireflective coating. (c) The 45° mirror facet at the waveguide end. (d) Waveguide entry facet and (e) waveguide S-bend of the interferometer.

MOEMS CHIP CHARACTERIZATION

The integrated MOEMS scanning chip is characterized in the measurement setup presented in Fig. 6a. The chip is wire-bonded to a customized printed circuit board (PCB) with contact pins (Fig. 6b) which is mounted to a customized holder to direct the light from the microlens towards the CCD camera. The light is brought to the chip from a 1.3 µm superluminescent light emitting diode (SLED) using a butt-coupled optical fiber. The fiber and waveguide entry facet are aligned using a digital optical microscope.

Figure 7 reports CCD images of the maximum displacement at operating current of 65 mA for the lateral and 55 mA for the vertical direction, respectively, with an acquisition time of 5 µs. Based on intensity calculation, no attenuation during device operation is observed.

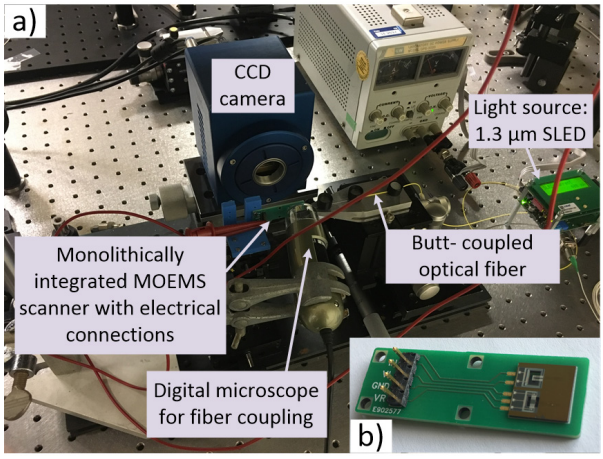

Figure 6: (a) Optical setup for device characterization. (b) MOEMS chip in a customized testing package.

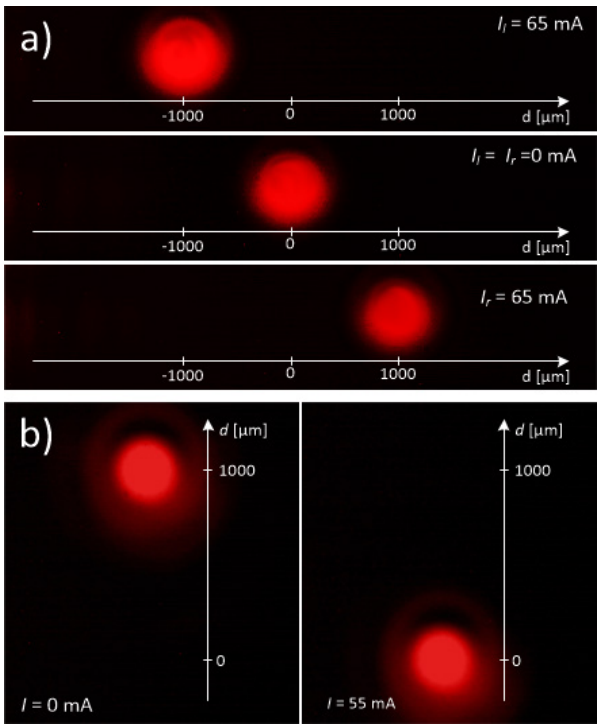

Figure 7: CCD images of MOEMS scanner light spot: (a) lateral scanning direction for (from top to bottom) left side actuated, unactuated and right side actuated light spot. (b) Vertical scanning direction in initial (left) and actuated state (right). The images were postprocessed to introduce false colors and increase the contrast for better visualization of the light spot.

A static measurement of the scanning range, at a working distance of 2 cm, versus driving current is presented in Fig. 8. A lateral scanning range of 2000 µm is

obtained, which corresponds to a 6° tilting motion range of the Si block (Fig. 8a), for an input current range of 0 mA to 65 mA on each actuator. The vertical MOEMS scanner provides a scanning range of 1000 µm for input current values between 0 mA and 55 mA (Fig. 8b). Mechanically, this corresponds to an angular displacement range of 3°. The average power consumption of the presented MOEMS systems is 170 mW, while the maximum error, as evidenced by the error bars in the graph, does not exceed 5% of the measured value.

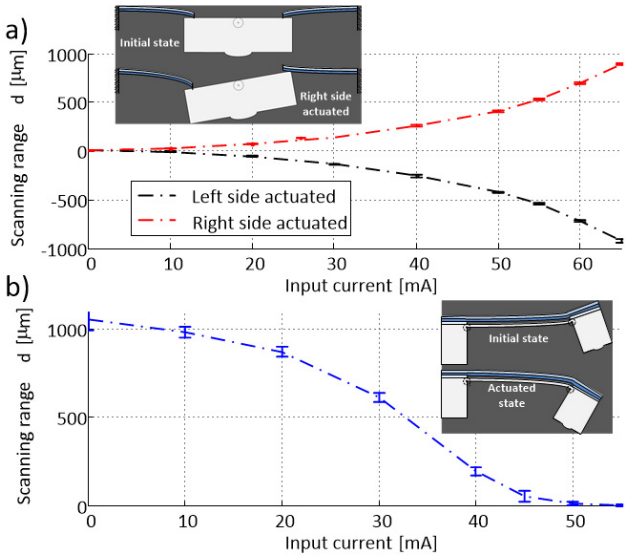

Figure 8: Scanning range at 2 cm working distance versus driving current for (a) lateral and (b) vertical direction scanning MOEMS device. The inset shows the working principle of the integrated MOEMS scanner.

CONCLUSION

The presented single-chip integrated MOEMS scanner provides a 2000 µm lateral and 1000 µm vertical scanning range, with an average output power of 170 mW. Within a footprint of only 7×10 mm^2 a passive photonic circuit for OCT interferometry is integrated with the presented MOEMS scanner. The components (waveguide, mirror, lens and actuators) are intrinsically-aligned during device fabrication. The microlens-collimated beam at the output of the interferometer allows the increase of the working distance to further extend the scanned surface range. This novel, highly miniaturized, single-chip, large scanning range MOEMS scanner paves the way towards innovative all-in-one chip imaging systems.

ACKNOWLEDGEMENTS

This research was funded by the EU (FP7-Project BiopsyPen nº 611132). The authors would like to thank the staff of the TU Delft Else Kooi Laboratory (previously DIMES) for help during device fabrication, Xin Yu of TU Delft and Zarko Zobenica of TU Eindhoven for assistance with the measurement setup

REFERENCES

[1] O. Solgaard, A. A. Godil, R. T. Howe, L. P. Lee, Y. A. Peter and H. Zappe, "Optical MEMS: From Micromirrors to Complex Systems", *Journal of Micromechanics and Microengineering*, Vol. 23, No. 3, pp. 517–537, 2014.

[2] S.H. Lee and Y.C. Lee, "Optoelectronic packaging for optical interconnects", *Optics and photonics news*, Vol. 17, Iss. 12, pp. 40-45, 2006.

[3] G. Yurtsever, P. Dumon, W. Bogaerts and R. Baets, "Integrated photonic circuit in silicon on insulator for Fourier domain optical coherence tomography", *Proc. SPIE 7554*, Optical Coherence Tomography and Coherence Domain Optical Methods in Biomedicine XIV, 75541B, 2010.

[4] E. Margallo-Balbas, M. Geljon, G. Pandraud and P. J. French, "Miniature 10 kHz thermo-optic delay line in silicon", *Optic Letters*, Vol. 35, No. 23, pp. 4027-4029, 2010.

[5] G. Pandraud, S. Milosavljevic, A. Sammak, M. Cherchi, A. Jovic and P. Sarro, "Integrated SiGe Detectors for Si Photonic Sensor Platforms", *Proceedings*, Vol. 1. No. 4. pp. 559, 2017.

[6] B. I. Akca, V. D. Nguyen, J. Kalkman, N. Ismail, G. Sengo, F. Sun, A. Driessen, T. G. van Leeuwen, M. Pollnau, K. Worhoff, and R. M. de Ridder, "Toward Spectral-Domain Optical Coherence Tomography on a Chip", *Journal of Selected Topics in Quantum Electronics*, Vol. 18, No. 3, pp. 1223-1233, 2012.

[7] T. Aalto, M. Harjanne, M. Kapulainena, S. Ylinena, M. Guinab, K. Haringb, J. Puustinenb, V. Mikhrinc, "GaAs-SOI integration as a path to low-cost optical interconnects", *Proc. SPIE 7941*, Integrated Optics: Devices, Materials, and Technologies XV, 79410S, 2011.

[8] S. Yoo, J. Y. Jin, J. G. Ha1, C. H. Ji and Y. K. Kim, "Two-dimensional optical scanner with monolithically integrated glass microlens", *Journal of Micromechanics and Microengineering*, Vol. 24, No. 5 pp. 055009, 2014.

[9] Y.H. Seo, K. Hwang, H. C. Park and K. H. Jeong, "Electrothermal MEMS fiber scanner for optical endomicroscopy", *Optic Express*, Vol. 24, No. 4, pp. 3904-3909, 2016.

[10] A. Jovic, G. Pandraud, K. Zinoviev, J. L. Rubio, E. Margallo, P. M. Sarro, "Fabrication process of Si microlenses for OCT systems", *Proc. SPIE 9888*, Micro-Optics, 98880C, 2016.

[11] A. Jovic, G. Pandraud, N.Sanchez, J. Sancho, K. Zinoviev, J. L. Rubio, E. Margallo and P. M. Sarro, "Two novel MEMS actuator systems for self-aligned integrated 3D optical coherent tomography scanners", in *2017 IEEE 30th International Conference on Micro Electro Mechanical Systems (MEMS),* Las Vegas, NV, 2017, pp. 797-800.

[12] Medlumics S.L., "Optical beam scanner", US9690093 B2, 2014.

CONTACT

*A. Jovic, tel: +31-615342385; a.jovic@tudelft.nl